http://dx.doi.org/10.5012/bkcs.2013.34.11.3327

Infrared Multiphoton Dissociation Spectroscopy of Protonated 1,2-Diaminoethane-water Clusters: Vibrational Assignment *via* the MP2 Method

Bong Hyun Boo,* Sukmin Kang, Ari Furuya,† Ken Judai,† and Nobuyuki Nishi†

*Department of Chemistry, Chungnam National University, Daejeon 305-764, Korea. *E-mail: bhboo@cnu.ac.kr*
†Institute for Molecular Science, Myodaiji, Okazaki 444-8545, Japan
Received July 31, 2013, Accepted August 24, 2013

Infrared multiphoton dissociation (IRMPD) spectra of various protonated 1,2-diaminoethane-water clusters DAE-H^+-$(H_2O)_n$ (n = 1-6) were measured in the wavelength range of 3000-3800 cm^{-1}. The IRMPD spectra of the well separated ionic clusters were simulated by the MP2 method employing various basis sets. Comparison of the IRMPD spectra with the theory indicates that each cluster may exist as several low-lying conformers, and the sum spectra of the various conformers reveal almost one to one correspondence between theory and experiment. Free N-H and O-H stretches are observed in the ranges of 3400-3500 and 3600-3800 cm^{-1}, respectively. The O-H···N and N-H···O stretches are, however, observed in the broad region of 3000-3600 cm^{-1}. The theoretical calculations on DAE-H^+-$(H_2O)_n$ (n = 1-4) show gradual decrease of the average binding energy between DAE-H^+ and H_2O as the cluster size increases, attaining the lowest value of 55 kJ/mol when n = 4. We found a low energy barrier of 21 kJ/mol to the isomerization converting the lowest energy cluster of DAE-H^+-H_2O to the second lowest one.

Key Words : Protonated 1,2-diaminoethane-water cluster, Infrared multiphoton dissociation, Simulated IR spectrum, Cluster binding energy

Introduction

Spectroscopic investigation on isolated molecules and clusters in conjunction with quantum mechanical MO calculation is quite informative as to the elucidation of both geometrical and vibrational structures and solvent effect. Generation of ultracold isolated hydrated clusters by utilizing the supersonic molecular beam technique permits the elucidation of state-to-state photophysics and cluster-size dependent photodissociation spectroscopy. The sophisticated technology also allows elimination of spectral broadening arising from collision effect in a bulk system and thus enables straightforward assignment of infrared photodissociation spectrum. Mass-selected photodissociation spectroscopy of protonated ion-water clusters in the gas phase is presumably one of the useful techniques for quantifying the vibrational energies and structures of isolated protonated hydrogen-bonded assemblies and for elucidating the presence of special proton site on the hydrated core molecule. For protonated 1,2-diaminoethane-water clusters of DAE-H^+-$(H_2O)_3$ (≡ DAE-H^+-W_3), geometrical and vibrational structures and interaction energies have been investigated by means of vibrational predissociation spectroscopy and ab initio calculation.[1] DAE molecule is relatively simple and volatile, and thus we can employ higher level theory by using large basis sets for quantum mechanical calculation and also experimentally we can generate relatively denser molecular beams.

The protonated DAE is well known to prefer a gauche form (~42 kJ/mol more stable) to a trans form.[2-5] The stability of a ring type conformation, in which the proton lies at the same distance from the two nitrogen atoms on the opposite sides, almost equals that of an open chain conformation where the proton attaches to one of two nitrogen atoms.[2] For DAE-H^+-W_3, the gauche form is also lower in energy than the trans form by 25-30 kJ/mol.[1,5] Variation of IRMPD spectra with cluster size is quite informative as to the elucidation of cluster stability, solvent effect, bonding sites, vibrational excitation and photodissociation behaviors. Our main purposes in the present study are: (1) to expand the cluster sizes of the hydrated complex ions such as DAE-H^+-W_n (n = 1-6) for the elucidation of cluster binding energy and spectral variation of the hydrated cluster with the cluster size; (2) to elucidate protonation efficiency of gas-phase hydrated DAE upon electron-impact ionization; (3) to investigate solvent effect on IRMPD spectrum by measuring a series of IRMPD spectra of protonated DAE-H^+-W_n (n =1-6); (4) to clarify hydration site on the core molecule *via* ab initio quantum-mechanical MO method; (5) to elucidate dissociation efficiency of vibrationally-excited protonated clusters being formed *via* the absorption of IR multiphoton by comparing the IRMPD spectra with the corresponding simulated IR spectra; (6) finally to search low energy reaction pathways for isomerizations of the solvated molecules by using the intrinsic reaction coordinate(IRC) analysis,[6-8] by which we can reliably obtain the transition states and also presumably find low-lying hydrated clusters.

Experimental and Computational Methodologies

The IRMPD spectra of DAE-H^+-W_n (n = 1-6) were measured by using the ion-guide spectrometer containing two

quadrupole mass filters. The construction and design of the mass spectrometer were detailed elsewhere[9,10] and also briefed here. A gas mixture of 1,2-diaminoethane, water, and argon was led to a vacuum chamber through a pulsed nozzle having a 0.80 mm orifice diameter and a 300 μs pulse duration. The total backing pressure was about 2×10^5 Pa. Neutral DAE-water binary clusters were ionized by electron-impact with an electron energy of *ca*. 350 eV near the exit hole of the pulsed nozzle. The protonated binary clusters formed were passed through a skimmer and then introduced into the spectrometer. Here, the ions, DAE-H^+-W_n (n = 1-6) of interest were selected by using the first quadrupole mass filter. After a 90° deflection through a ion bender, the parent ions were led into a quadrupole ion beam guide. The cluster ion beam was crossed with a laser beam in the ion guide, and then the parent ions were jumped into vibrationally excited state and dissociated thereafter. Resultant daughter ions were mass-analyzed by the second quadrupole mass filter. For the normalization of the fragment-ion yield, the laser power was monitored by a pyroelectric detector. IRMPD spectra were obtained by plotting the normalized yields of the daughter ions vs. the wavenumbers of the dissociation laser. A tunable infrared source was an optical parametric oscillator (OPO) system pumped with an injection-seed Nd:YAG laser. The output energy used in this experiment was 1-2 mJ/pulse. The linewidth was approximately 1 cm^{-1}. The wavenumber of the infrared laser was calibrated by a commercial wavemeter.

All the calculations were carried out with the Gaussian 09 package suite.[11] We assembled the cluster geometries by putting a water molecule one by one around the ionic core of DAE-H^+. It means that after the optimization of DAE-H^+, we added one water molecule into the lowest structure of DAE-H^+ to attain maximum hydrogen bond energy. The ground-state equilibrium geometries and energies of DAE-H^+-W_n (n = 1-4) were probed by the MP2/cc-pVTZ[12-15] or MP2/6-311+G(d,p) methods, depending on the cluster size. For each structure, the complete sets of harmonic vibrational frequencies were then calculated with the analytical second derivative technique by using the MP2/6-311+G(d,p) or MP2/6-31G(d) method. Note that one should employ similar calculation level and basis set in both of the electronic and vibrational energy calculations to obtain energies of the relaxed optimized geometries. And thus we totally employed the MP2 method by using the similar basis sets to calculate both of the electronic and vibrational energies. Because the simulated spectra are found to be very sensitive to the geometrical structures of the clusters, and thus, we employed the MP2 method, which takes into account of dispersion effectively for the structural optimization. MP2 dispersion should be particularly considered in the weakly bound cluster. The harmonic vibrational frequencies were also used to determine whether a given structure is a local minimum on the potential energy surface or not. Note that inner-shell electrons were excluded in the electron-correlation calculation to reduce the computational time. The zero-point corrections were made to the electronic energies by using a scale factor of 0.947, the value evaluated in the present study. Thermal corrections were also made to the energies and Gibbs free energies. Some of the simple reaction pathways involving the migration of one water molecule were confirmed by carrying out the IRC analysis,[6-8] by which we could check whether or not the geometries of the reactants and products used for the prediction of the transition states are correctly reproduced.

Results and Discussion

Figure 1 presents mass spectra of the ionic clusters corresponding to H^+-W_m (m = 4-9) and DAE-H^+-W_n (n = 0-6) where the W letter refers to a water molecule. As seen in Figure 1, the presence of the mass to charge ratios corresponding to 61, 79, 97 clearly indicates that protonated DAE-water clusters are formed in the electron impact ionization source. The intramolecular hydrogen-bond energy of protonated DAE was computed to be relatively large as 29 kJ/mol with the MP2/D95V** method,[2] and thus, the protonation is presumably a feasible process in the electron-impact ionization of the DAE-water clusters. It is unknown why the mass spectral peaks appears as doublets. Note that we showed the mass spectrum in the three regions having different intensity scale because the cluster mass intensity decreases considerably with increasing the cluster size. Propensity of particular cluster ion in abundance is not found in the present heterocluster system involving DAE-H^+-W_n (n = 0-6) and the homocluster one associated with H^+-W_m (m = 4-9).

Figure 2 presents IRMPD spectra of DAE-H^+-W_n (n = 1-6) measured in the range 3000-3800 cm^{-1}. We found that our IRMPD spectra were well reproducible in the our several experiments, and especially the spectrum for DAE-H^+-W_3 also matches well with a previously reported one.[1] Figures 3-6 compare the IRMPD spectra of DAE-H^+-W_n (n = 1-4) with the corresponding simulated IR spectra evaluated with the MP2 level by using the various basis sets. When the

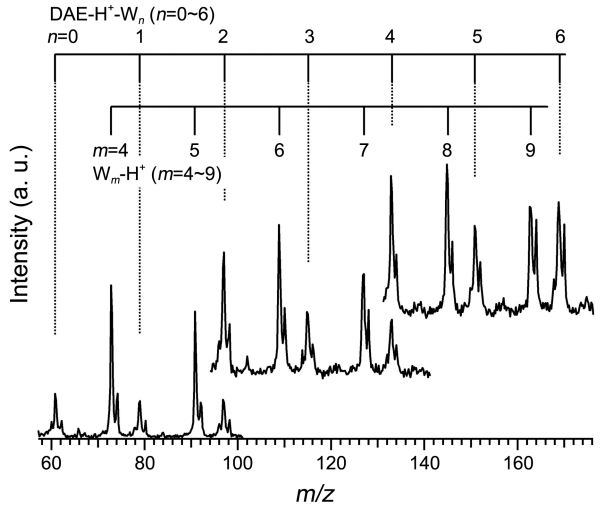

Figure 1. Mass spectra of protonated 1,2-diaminoethane-water clusters DAE-H^+-W_n (n = 0-6) and protonated water clusters H^+-W_m (m = 4-9).

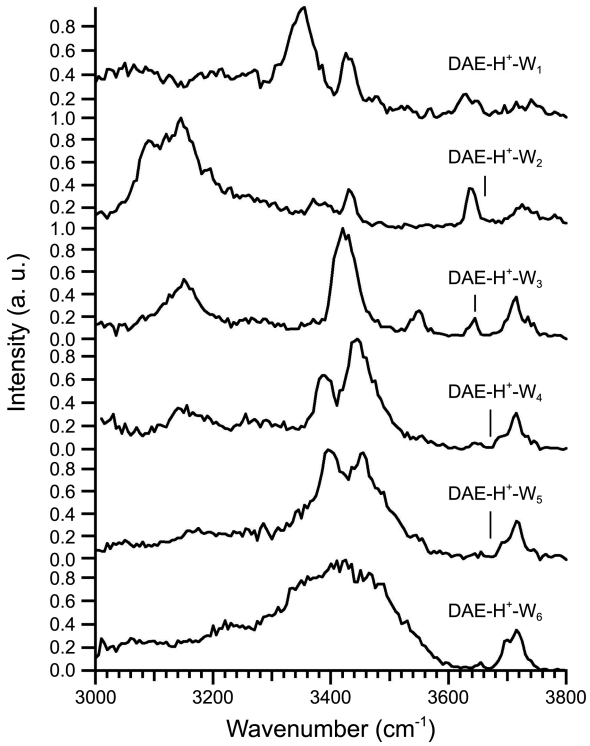

Figure 2. IRMPD spectra of protonated 1,2-diaminoethane-water clusters DAE-H^+-W_n (n = 1-6).

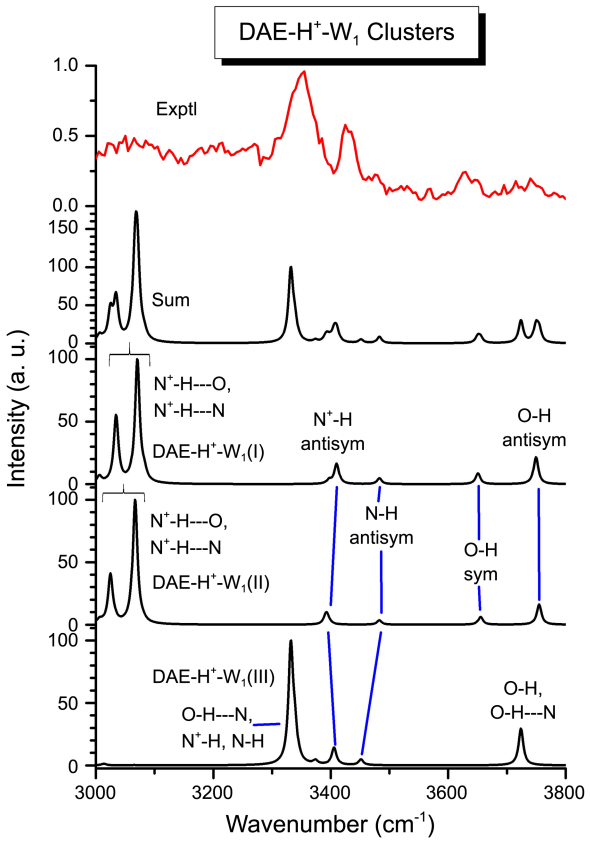

Figure 3. IRMPD spectrum of protonated 1,2-diaminoethane-water clusters DAE-H^+-W_1 is compared with the corresponding simulated infrared spectra evaluated with the MP2/6-311+G(d,p)//MP2/cc-pVTZ method and with the sum spectrum.

vibrational frequencies were scaled by 0.947, the rms deviation from experiment turns out to be as small as 24.7 cm^{-1}. Note that the simulated spectra have a Lorentzian distribution having a fwhm of 10 cm^{-1}. The usage of the relatively broad bandwidth is found to reproduce the relatively broad vibrational peaks presumably arising from the multiphoton dissociation of the protonated clusters. In our previous studies, Lorentzian line functions having a small bandwidth of 4.0 cm^{-1} match very well with experimental IR spectra of even solid hydrocarbon compounds.[16,17] Also note that there is no physical meaning in the usage of the 10 cm^{-1} bandwidth.

Figure 3 compares the IRMPD spectrum for DAE-H^+-W_1 with the simulated IR spectra of the low-lying conformers (for the geometries, see Figure 7(a)) evaluated with the MP2/6-311+G(d,p)//MP2/cc-pVTZ method. The experimental spectrum is found to match well with the sum of the simulated IR spectra of three low-lying conformers. Note that the sum spectrum is achieved with the summation of the three individual spectra with equal propensity. Also note that unawareness of the cluster beam temperature hampers the application of the Boltzmann distribution by which we can evaluate relative propensity of the three low-lying isomers. We presume that thermal equilibrium condition is not applicable in the cluster beam system involving the supersonic expansion. Tables 1-2 list energies and Gibbs free energies of the various low-lying complexes. We searched three low-lying conformers corresponding to each DAE-H^+-W_n (n = 1-4). Note that the Roman numerals indicate the order of the relative total Gibbs free energies. The lowest energy conformer is DAE-H^+-W_1(I). We presume that the other two clusters of DAE-H^+-W_1(II) and DAE-H^+-W_1(III) also contribute to the total experimental spectrum of DAE-H^+-W_1 because the Gibbs free energies of the two clusters are slightly higher than DAE-H^+-W_1(I) by only about 5 and 21 kJ/mol, respectively.

Figure 4 compares the IRMPD spectrum for DAE-H^+-W_2 with the corresponding simulated IR spectra for DAE-H^+-W_2 (X) (X = I, II, III) evaluated with the MP2/6-311+G(d,p)//MP2/6-311+G(d,p) method. The N-H and O-H stretches are experimentally observed in the ranges of 3400-3500 and 3600-3800 cm^{-1}, respectively. The H-bonded O-H stretches (O-H···N) are observed in the broad region of 3400-3500 cm^{-1}. On the other hand, the H-bonded N-H stretches (N^+-H···O and N^+-H···N) are observed in the broad region of 3000-3200 cm^{-1}. Figure 5 compares the IRMPD spectrum of DAE-H^+-W_3 with the simulated spectra of DAE-H^+-W_3 (X) (X = I, II, III) evaluated with the MP2/6-311+G(d,p)//MP2/6-311+G(d,p) method. The individual simulated spectra of the low-lying conformers of DAE-H^+-W_3 (X) (X = I, II, III) are found to match with the corresponding IRMPD spectrum. Moreover, the sum spectrum also matches well with the experimental spectrum. It is shown theoretically that the relative intensity for the free O-H stretch gradually decreases whereas those of O-H···N and O-H···O stretches gradually

Table 1. Electronic, zero-point, and the relative energies of the various clusters DAE-H^+-W_n (n = 0-2) calculated at the MP2 level using the various basis sets[a]

Conformer	Electronic energy in au	Zero-point energy in au[b]	Therm. corr. to energy 298.15 K In kJ/mol[c]	Therm. corr. to Gibbs free energy 298.15 K In kJ/mol[d]
	MP2/cc-pVTZ //MP2/cc-pVTZ	MP2/6-311+G(d,p) //MP2/cc-pVTZ	MP2/6-311+G(d,p) //MP2/cc-pVTZ	MP2/6-311+G(d,p) //MP2/cc-pVTZ
DAE-H^+-gauche	-190.514595 (0)[e] (0)[f]	0.121032	13.7	-71.9
DAE-H^+-trans	-190.497322 (43.7) (40.4)	0.120153	14.4	-74.6
	MP2/cc-pVTZ //MP2/cc-pVTZ	MP2/6-311+G(d,p) //MP2/cc-pVTZ	MP2/6-311+G(d,p) //MP2/cc-pVTZ	MP2/6-311+G(d,p) //MP2/cc-pVTZ
DAE-H^+-W_1(I)	-266.862051 (1.9) (0)	0.144134	21.0	-87.7
DAE-H^+-W_1(II)	-266.861758 (0) (5.4)	0.143872	19.0	-82.4
DAE-H^+-W_1(III)	-266.858553 (11.0) (20.8)	0.145153	18.2	-78.8
	MP2/cc-pVTZ //MP2/6-311+G(d,p)	MP2/6-311+G(d,p) //MP2/6-311+G(d,p)	MP2/6-311+G(d,p) //MP2/6-311+G(d,p)	MP2/6-311+G(d,p) //MP2/6-311+G(d,p)
DAE-H^+-W_1(TS)[g]	-266.854373 (20.9) (18.7)	0.143560	21.3	-87.7
	MP2/6-311+G(d,p) //MP2/6-311+G(d,p)	MP2/6-311+G(d,p) //MP2/6-311+G(d,p)	MP2/6-311+G(d,p) //MP2/6-311+G(d,p)	MP2/6-311+G(d,p) //MP2/6-311+G(d,p)
DAE-H^+-W_2(I)	-342.991446 (0) (0)	0.166894	32.6	-103.9
DAE-H^+-W_2(II)	-342.988560 (10.7) (14.6)	0.167852	30.3	-99.0
DAE-H^+-W_2(III)	-342.989339 (17.3) (33.5)	0.168450	29.2	-95.8

[a]Zero-point energies and thermal energies (excluding *ZPE*) were corrected to the electronic energies as $E_{total} = E_{el} + ZPE + E_{th}$ and to the Gibbs free energies as $G_{total} = E_{el} + ZPE + E_{th} + pV - TS \equiv E_{el} + ZPE + G_{th}$. [b]The *ZPE* was scaled by 0.947. [c]The thermal energy is the sum of translational, rotational and vibrational energies at 298.15 K excluding the *ZPE*. [d]Contribution from translational, rotational and vibrational energies at 298.15 K (except the *ZPE*), $\Delta(pV)(= RT)$, and $-TS$ where T = 298.15 K and $S = S_{298.15\ K}$, *i.e.*, $G_{th} = E_{th} + pV - TS$. [e]The values denoted in the first parentheses refer to the relative total energies in kJ/mol. [f]The values denoted in the second parentheses refer to the relative Gibbs free energies in kJ/mol. [g]It was found in the IRC analysis that the transition state is connected to the low-lying clusters of DAE-H^+-W_1(I) and DAE-H^+-W_1(II).

increase as the cluster size increases.

Figure 6 compares the IRMPD spectrum for DAE-H^+-W_4 with the corresponding simulated IR spectra for DAE-H^+-W_4 (X) (X = I, II, III) evaluated with the MP2/6-31G(d)// MP2/6-311+G(d,p) method. The sum spectra of the simulated spectra of low-lying conformers for DAE-H^+-W_4 (X) (X = I, II, III) are found to match with the IRMPD spectrum. The experimental spectrum seems to consist of three regions. The free symmetric O-H stretch is presumed to be immersed in the O-H···N and O-H···O stretches. The IRMPD spectra of DAE-H^+-W_n (n = 1-6) reveal that there are almost three regions of the infrared absorptions: (1) 3600-3800 cm^{-1} corresponding to free O-H vibration; (2) 3300-3600 cm^{-1} arising from free N-H and O-H···O vibrations; (3) 3000-3300 cm^{-1} corresponding to N-H···N, N-H···O, and free C-H stretches. The variation of the IRMPD spectra with the cluster size is significant, revealing that the intensities of the free O-H stretching intensity and the H-bonded N^+-H···O stretching one are significantly diminished with increasing the cluster size. This is because the free O-H and N^+-H···O stretching density of state are getting less than the O-H···O one as the cluster size increases. It is also clearly shown in

Table 2. Electronic, zero-point, and the relative energies of the various clusters DAE-H^+-W_n (n = 3-4) calculated at the MP2 level using the various basis sets[a]

Conformer	Electronic energy in au	Zero-point energy in au	Therm. corr. to energy 298.15 K In kJ/mol	Therm. corr. to Gibbs free energy 298.15 K In kJ/mol
	MP2/6-311+G(d,p) //MP2/6-311+G(d,p)	MP2/6-311+G(d,p) //MP2/6-311+G(d,p)	MP2/6-311+G(d,p) //MP2/6-311+G(d,p)	MP2/6-311+G(d,p) //MP2/6-311+G(d,p)
DAE-H^+-W_3(I)	-419.289258 (0) (0)	0.192200	37.9	-109.1
DAE-H^+-W_3(II)	-419.285436 (10.7) (14.6)	0.192932	36.6	-106.4
DAE-H^+-W_3(III)	-419.287897 (4.3) (16.4)	0.194014	33.8	-100.9
	MP2/6-311+G(d,p) //MP2/6-311+G(d,p)	MP2/6-31G(d) //MP2/6-311+G(d,p)	MP2/6-31G(d) //MP2/6-311+G(d,p)	MP2/6-31G(d) //MP2/6-311+G(d,p)
DAE-H^+-W_4(I)	-495.582718 (8.2) (0)	0.214517	38.6	-113.3
DAE-H^+-W_4(II)	-495.584156 (0) (2.8)	0.214364	34.6	-106.3
DAE-H^+-W_4(III)	-495.583568 (9.8) (8.4)	0.216684	36.7.	-108.4

[a]The various notations described in Table 2 are the same as indicated in the footnotes in Table 1.

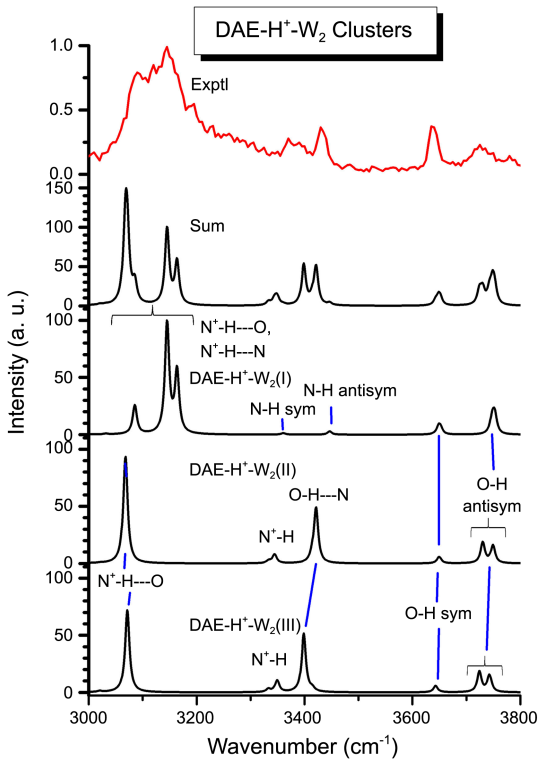

Figure 4. IRMPD spectrum of protonated 1,2-diaminoethane-water clusters DAE-H^+-W_2 is compared with the corresponding simulated infrared spectra evaluated with the MP2/6-311+G(d,p)// MP2/6-311+G(d,p) method and with the sum spectrum.

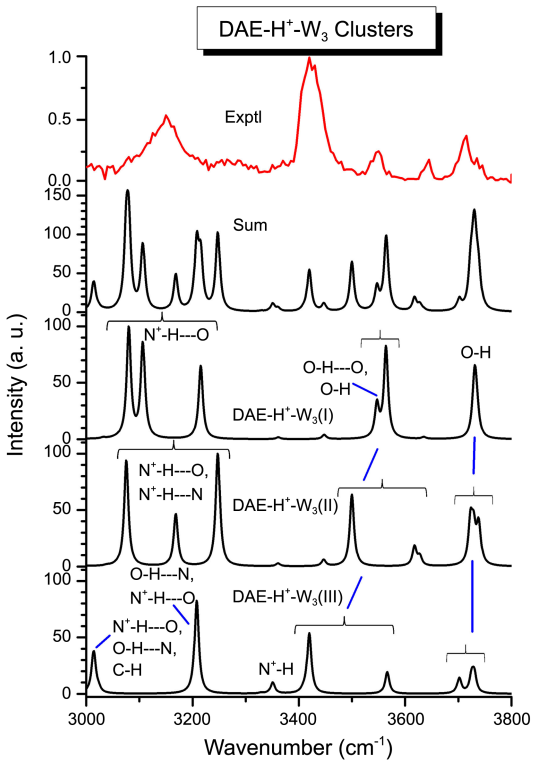

Figure 5. IRMPD spectrum of protonated 1,2-diaminoethane-water clusters DAE-H^+-W_3 is compared with the corresponding simulated infrared spectra evaluated with the MP2/6-311+G(d,p)// MP2/6-311+G(d,p) method and with the sum spectrum.

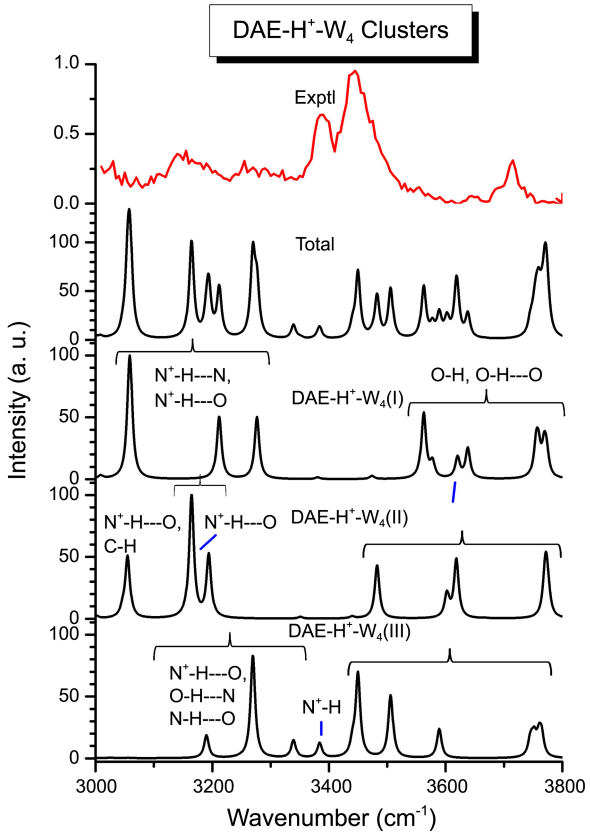

Figure 6. IRMPD spectrum of protonated 1,2-diaminoethane-water clusters DAE-H^+-W_4 is compared with the corresponding simulated infrared spectra evaluated with the MP2/6-31G(d)//MP2/6-311+G(d,p) method and with the sum spectrum.

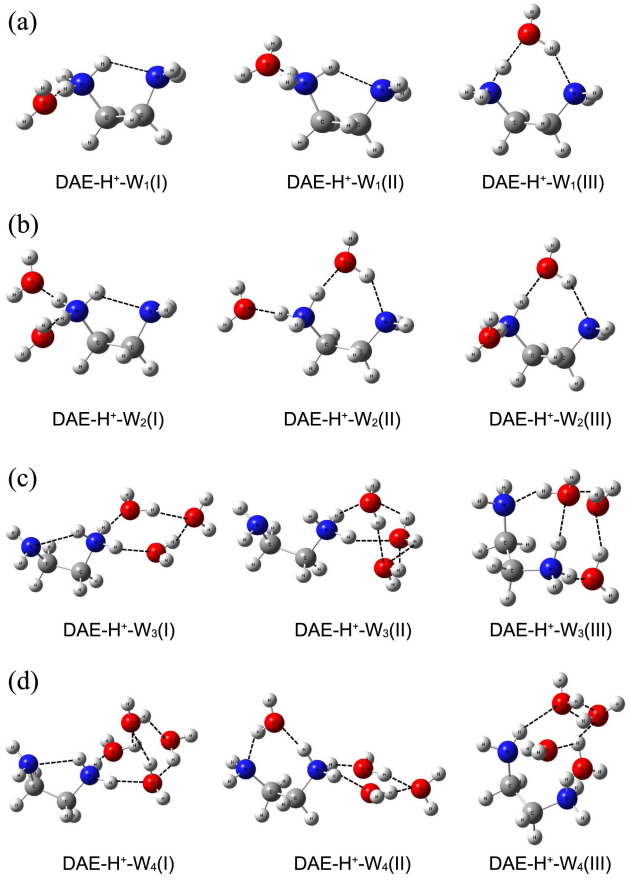

Figure 7. Molecular models of low-lying protonated 1,2-diamino-ethane-water clusters DAE-H^+-W_n (n = 1-4) optimized with the MP2/cc-pVTZ (for n = 1) or MP2/6-311+G(d,p) (for n = 2-4) methods.

the IRMPD spectra that as the cluster size increases, the intensity for the free antisymmetric O-H stretch decreases, and the O-H···O and O-H···N stretching peaks are relatively getting broader and higher. The simulated infrared spectra of the low-lying clusters evaluated with the MP2/6-311+G(d,p) or MP2/6-31G(d) method at the geometries optimized with the MP2/cc-pVTZ or MP2/6-311+G(d,p) methods are found to partially contribute to the IRMPD spectrum of the corresponding cluster. This implies that each cluster exists as the corresponding several conformers at the beam temperature used in the present study.

Figure 7 presents molecular models for the low-lying DAE-H^+-W_n (n = 1-4). The conformers having a N-H···N framework (the gauche geometry) are found to be lowest in all the protonated binary clusters. Note that the proton does not lie at the same distance from the two nitrogen atoms. However, their simulated IR spectra are found to be only a part of the experimental spectra. This can be taken as an implication that in one given cluster, there exist low-lying several conformers. Our theoretical calculations using the MP2/cc-pVTZ method also indicate that the gauche form of the protonated DAE is more stable by 40 kJ/mol (ΔG, ΔE = 44 kJ/mol), in excellent agreement with the reported values.[2-5] By using the theoretical data listed in Tables 1-3, we derived average binding energies corresponding to the lowest conformers of DAE-H^+-W_n (n = 1-4. We also observe gradual decrease of the average binding energies between DAE-H^+ and H_2O as the cluster size increases, attaining the lowest value of 55 kJ/mol when n = 4. This kind of energetic behavior was also reported experimentally in a previous work performed by Belau *et al.* who evaluated dissociation energies of neutral water clusters.[18] They also found the gradual decrease of the cluster binding energy for $(H_2O)_n$ (n = 3-9) → $(H_2O)_{n-1}$ (n = 3-9) + H_2O as the n increases. Recently, Romero *et al.* studied theoretically structures and energies of lithium ion-water clusters $(H_2O)_nLi^+$(n = 3-5).[19] They analyzed total cluster binding energy in terms of solute-solvent and solvent-solvent interactions, and revealed that the solute-solvent interactions are major stabilizing interactions for the clusters.

In an attempt to perform reliability test of checking whether the low-lying clusters whose structures were optimized in the present study are really low or not , we achieved several transition states and then checked that the clusters are appropriately connected to the transition state by using the IRC analysis. During the procedure, we searched some low-lying clusters. As listed in Table 1, we obtained low-lying reaction pathways for the shift of one solvated water molecule involving the transition state DAE-H^+-W_1(TS) which

Table 3. Electronic and zero-point energies, and thermal corrections of protonated 1,2-diaminoethane and water molecule calculated at the MP2 level using the various basis sets[a]

Conformer	Electronic energy in au	Zero-point energy in au	Therm. corr. to energy 298.15 K In kJ/mol	Therm. corr. to Gibbs free energy 298.15 K In kJ/mol
	MP2/cc-pVTZ //MP2/cc-pVTZ	MP2/6-311+G(d,p) //MP2/cc-pVTZ	MP2/6-311+G(d,p) //MP2/cc-pVTZ	MP2/6-311+G(d,p) //MP2/cc-pVTZ
H_2O	-76.318658	0.020548	7.4	-46.3
DAE-H^+	-190.514595	0.121032	13.7	-71.9
	MP2/6-311+G(d,p) //MP2/6-311+G(d,p)	MP2/6-311+G(d,p) //MP2/6-311+G(d,p)	MP2/6-311+G(d,p) //MP2/6-311+G(d,p)	MP2/6-311+G(d,p) //MP2/6-311+G(d,p)
H_2O	-76.274720	0.020526	7.4	-46.3
DAE-H^+	-190.389620	0.120804	13.2	-71.3
	MP2/6-311+G(d,p) //MP2/6-311+G(d,p)	MP2/6-31G(d) //MP2/6-311+G(d,p)	MP2/6-31G(d) //MP2/6-311+G(d,p)	MP2/6-31G(d) //MP2/6-311+G(d,p)
H_2O	-76.274720	0.020844	7.4	-46.3
DAE-H^+	-190.389620	0.122315	13.3	-71.5

[a]The various notations described in Table 3 are the same as indicated in the footnotes in Table 1.

Table 4. Average binding energies between DAE-H^+ and H_2O at 298.15 K in the various lowest-energy clusters derived from the data listed in Tables 1-3

Conformer	Average binding energy ($D^0_{298.15}$) in kJ/mol
DAE-H^+-W_1(I)	69.0
DAE-H^+-W_2(I)	61.9
DAE-H^+-W_3(I)	56.7
DAE-H^+-W_4(I)	55.3

separates the low-lying clusters of DAE-H^+-W_1(I) and DAE-H^+-W_1(II), the energy barrier for which is found to be as low as 21 kJ/mol. It is very intriguing to energetically interpret the observed IRMPD spectra. As listed in Table 4, the average bond energy between DAE-H^+- and H_2O is evaluated to be the lowest value of 55 kJ/mol when n = 4, which corresponds to 4600 cm^{-1}. The single photon energy ranging from 3000 to 3800 cm^{-1} used in the present study is not enough to detach one water molecule from the clusters. Therefore, we presume that multiphoton dissociation event leads to the observation of the present spectra. The multiphoton absorption leading to the detachment of one molecule from the clusters gives rise to the broadening of the IRMPD spectra. It is not known whether for example in the two-photon absorption case, resonant two-photon vibrational excitation or resonant one-photon excitation followed by another photon absorption takes place. We presume that these two events eventually bring up the ITMPD spectral broadening.

Conclusions

We successfully generated various jet-cooled protonated 1,2-diaminoethane-water clusters DAE-H^+-W_n (n = 1-6), the IRMPD spectra for which were measured in the range of 3000-3800 cm^{-1}. The IRMPD spectra of the simple isolated clusters were then compared with the corresponding simulated IR spectra evaluated with the MP2 method using the various basis sets of 6-31G(d), 6-311+G(d,p), and cc-pVTZ. The sum spectrum of the corresponding simulated IR spectra of the low-lying clusters are found to match well with the IRMPD spectra. The free N-H and O-H stretches are observed in the ranges of 3400-3500 cm^{-1} and 3600-3800 cm^{-1}, respectively. However, The N-H···O and O-H···O stretches are observed in the low and broad region of 3000-3600 cm^{-1}. The lowest energy conformers are found to include a five-membered ring, in which the proton lies between the two nitrogen atoms, but not at the same distance from the two nitrogen atoms. The MP2 calculations on DAE-H^+-W_n (n = 1-4) show gradual decrease of the average binding energy between for DAE-H^+ and H_2O as the cluster size increases, attaining the lowest value of 55 kJ/mol when the four water molecules are hydrated around the central DAE molecule. We searched a transition state in the isomerization of DAE-H^+-W_1(I) to DAE-H^+-W_1(II), the activation energy for which is found to be as low as 21 kJ/mol.

References

1. Kim, K.-Y.; Chang, H.-C.; Lee, Y. T.; Cho, U.-I.; Boo, D. W. *J. Phys. Chem. A* **2003**, *107*, 5007, references therein.
2. Ikuta, S.; Nomura, O. *J. Mol. Struct. (Theochem)* **1987**, *37*, 315.
3. Ikuta, S.; Nomura, O. *Chem. Phys. Lett.* **1989**, *154*, 71.
4. Yamabe, S.; Hirao, K.; Wasada, H. *J. Phys. Chem.* **1992**, *96*, 10261.
5. Boo, D. W. *Bull. Korean Chem. Soc.* **2001**, *22*, 693.
6. Fukui, K. *Acc. Chem. Res.* **1981**, *14*, 363.
7. Gonzales, C.; Schlegel, H. B. *J. Chem. Phys.* **1989**, *90*, 2154.
8. Gonzales, C.; Schlegel, H. B. *J. Phys. Chem.* **1990**, *94*, 5523.
9. Kosugi, K.; Inokuchi, Y.; Nishi, N. *J. Chem. Phys.* **2001**, *114*,

4805.
10. Inokuchi, Y.; Nishi, N. *J. Chem. Phys.* **2001**, *114*, 7059.
11. Frisch, M. J.; Trucks, G. W.; Schlegel, H. B.; Scuseria, G. E.; Robb, M. A.; Cheeseman, J. R.; Scalmani, G.; Barone, V.; Mennucci, B.; Petersson, G. A.; Nakatsuji, H.; Caricato, M.; Li, X.; Hratchian, H. P.; Izmaylov, A. F.; Bloino, J.; Zheng, G.; Sonnenberg, J. L.; Hada, M.; Ehara, M.; Toyota, K.; Fukuda, R.; Hasegawa, J.; Ishida, M.; Nakajima, T.; Honda, Y.; Kitao, O.; Nakai, H.; Vreven, T.; Montgomery, J. A., Jr.; Peralta, J. E.; Ogliaro, F.; Bearpark, M.; Heyd, J. J.; Brothers, E.; Kudin, K. N.; Staroverov, V. N.; Kobayashi, R.; Normand, J.; Raghavachari, K.; Rendell, A.; Burant, J. C.; Iyengar, S. S.; Tomasi, J.; Cossi, M.; Rega, N.; Millam, J. M.; Klene, M.; Knox, J. E.; Cross, J. B.; Bakken, V.; Adamo, C.; Jaramillo, J.; Gomperts, R.; Stratmann, R. E.; Yazyev, O.; Austin, A. J.; Cammi, R.; Pomelli, C.; Ochterski, J. W.; Martin, R. L.; Morokuma, K.; Zakrzewski, V. G.; Voth, G. A.; Salvador, P.; Dannenberg, J. J.; Dapprich, S.; Daniels, A. D.; Farkas, ?.; Foresman, J. B.; Ortiz, J. V.; Cioslowski, J.; Fox, D. J. *Gaussian 09*, Revision A. 1; Gaussian, Inc.; Wallingford CT, 2009.
12. Dunning, T. H., Jr. *J. Chem. Phys.* **1989**, *90*, 1007.
13. Kendall, R. A.; Dunning, T. H., Jr.; Harrison, R. J. *J. Chem. Phys.* **1992**, *96*, 6796.
14. Wilson, A. K.; van Mourik, T.; Dunning, T. H., Jr. *J. Mol. Struct.* (*Theochem*) **1996**, *388*, 339.
15. Davidson, E. R. *Chem. Phys. Lett.* **1996**, *260*, 514.
16. Boo, B. H.; Lee, S. Y.; Na, H.-K. *J. Phys. Chem. A* **1998**, *102*, 2679.
17. Boo, B. H.; Park, J.; Yeo, H. G.; Lee, S. Y.; Park, C. J.; Kim, J. H. *J. Phys. Chem. A* **1998**, *102*, 1139.
18. Belau, L.; Wilson, K. R.; Leone, S. R.; Ahmed, M. *J. Phys. Chem. A* **2007**, *111*, 10075.
19. Romero, J.; Reyes, A.; David, J.; Restrepo, A. *Phys. Chem. Chem. Phys*. **2011**, *13*, 15264.